CHEMICAL ENGINEERING TRANSACTIONS
VOL. 35, 2013
A publication of AIDIC
The Italian Association of Chemical Engineering
www.aidic.it/cet
Guest Editors: Petar Varbanov, Jiří Klemeš, Panos Seferlis, Athanasios I. Papadopoulos, Spyros Voutetakis

ISBN 978-88-95608-26-6; **ISSN** 1974-9791
DOI: 10.3303/CET1335120

Effect of the Type of Impellers on Mixing in an Electrochemical Reactor

Helvio Mollinedo[a], Jorge Ramírez [b], Oliver Huerta [c], Victor X. Mendoza[d], Sergio A. Martínez*[,e]

[a]UPIITA, Instituto Politécnico Nacional. Av.IPN 2580, Ticoman. México D.F. México.
[b]Depto. Energia,. Universidad Autónoma Metropolitana Azcapotzalco. Av. San Pablo 180. Azcapotzalco. CP 07740, México D.F. México.
[c]SEPI. ESIME, Instituto Politécnico Nacional. U. P. Ticomán. México D.F. Mexico
[d]Depto. Electronica,. Universidad Autónoma Metropolitana Azcapotzalco. Av. San Pablo 180. Azcapotzalco. CP 07740, México D.F. México.
[e]Depto. Ciencias Básicas, Universidad Autónoma Metropolitana Azcapotzalco. Av. San Pablo 180. Azcapotzalco. CP 07740, México D.F. México.
samd@correo.azc.uam.mx

The electrochemical process is an alternative method to remove hexavalent chromium Cr(VI) from industrial wastewaters process. However, in electrochemical plug flow reactors with no liquid mixing or static electrodes, iron salt film is formed on the electrodes surface (electrode passivation) because of the poor diffusion and mass transfer that reduces the Cr (VI) removal efficiency and causes greater energy consumption. Therefore, the electrochemical reactors require to be designed to provide high mass transfer between the bulk liquid and the electrodes. Electrochemical reactors with electrodes such as the rotating electrodes have been studied to reduce the passivation effect. It has been demonstrated that in this kind of electrochemical reactors, the flow velocity field and turbulence intensity are not and there is a zone inside the rotating ring electrodes, about 35 % of the reactor volume, with low velocity, turbulence and vorticity that reduces the mass transfer and process efficiency. In this study, the performance of two kinds of impellers (four internal fins and one internal pitched blade turbine) located inside the ring electrodes zone were evaluated in an electrochemical reactor with rotating ring electrodes with a volume capacity of 18 L. Their performance was compared with the reactor without impellers inside the ring electrode. Experimental test at different rotational speeds were performed with both kind of impellers to evaluate the mixing time and the power consumption. CFD tools were used to describe their performance. The mixing time was reduced up to 33 % for the 4 internal fins reactor and 52 % with the pitched blade central (PB4) turbine in comparison with rotating ring electrode without internal impellers. The highest mean turbulence intensity and vorticity was reached with the pitched blade central turbine and the power consumption was the same in all the cases.

1. Introduction

In the electrochemical processes with sacrifice electrodes, an oxide fouling film is formed on the electrodes surface that reduces the process efficiency and increases the power consumption (Martinez et al., 2000). To reduce the passivation effect, other researchers have been devoted their efforts to explore other kind of the electrochemical reactors with electrodes such as the rotating electrodes (Martinez et al. 2011; Martinez et al. 2012). In those works, the effect of the rotating ring electrode speeds was evaluated. It was found that as the rotational electrode speed increased, the treatment time was reduced. However, at the higher rotational speeds studied (i.e.150 rpm and 230 rpm) there was not important effect in the reduction of the treatment time, which was due to the behaviour of the fluid inside the rotating ring electrodes zones was very similar, in spite of the rpm of the rotating electrodes was increased (Martinez et al., 2013).. By using CFD tools, it was possible to found that in this zone, the magnitude velocity and the

Please cite this article as: Mollinedo H., Ramirez J., Huerta O., Mendoza V.X., Martinez S.A., 2013, Effect of the type of impellers on mixing in an electrochemical reactor, Chemical Engineering Transactions, 35, 721-726 DOI:10.3303/CET1335120

turbulent intensity was similar. Due to this effect, the transport of the reactants throughout the reactor was limited; causing that the increase in the rpm had no important effect on the electrochemical reaction rate. Based in the combination of experimental and CFD tools, it has been possible to have better understanding of the mixing process inside the reactors and it has been possible to determine different parameters as the velocity field, the vorticity, turbulent intensities, and circulation patterns, among others. It is well known that the efficiency of a reactor depends mainly on their geometrical configuration: the shape of the tank, the type and number of impellers, and the number of baffles (Rammohan et al., 2001). In this work, to increase the mixing and mass transference throughout the reactor and reduce the zones with low vorticity and turbulence that exist inside the electrode rings zone, two kinds of impellers were evaluated; one with four internal fins (4 fins) and the other, with internal pitched blade (PB4) turbine. In both cases the impellers were located inside the ring electrodes zone and they rotated at the same rpm´s than the ring electrode. The reactor performance was carried out at different rotational speeds (75 rpm, 150 rpm and 230 rpm) to evaluate their effect on the processes. The electrochemical reactor with has a volume capacity of 18 L and the fluid behaviour inside the reactor was evaluated by the state-of the-art computational fluid dynamics (CFD) tools.

2. Methods

2.1 Numerical simulation

The numerical simulation was performed using specialized software CFD Fluent©. A complete three dimensional model were prepared for each geometrical configuration of the reactor. Due to the complex geometrical shapes, all these models were meshed using tetrahedral cells. The grid independence was taken into account by considering the balance between mesh density and computational resources, comparing them with simulations of the same reactor models reported in previous work (Martinez, 2012).

The CFD simulations were performed using a pressure-based segregated algorithm solver, where the governing equations are solved sequentially. For the discretization of the governing equations, the standard scheme was selected for pressure discretization, while a second order upwind scheme was used for momentum discretization, and for the pressure-velocity coupling, the semi implicit pressure-linked equation (SIMPLE) algorithm was used. During simulation has been solved the most recently developed of the three κ-ε variations turbulence model called Realizable. Realizable κ-ε model has two main differences from the κ-ε model standard, the first one uses a new equation for the turbulent viscosity and the dissipation rate transport equation has been derived from the equation for the transport of the mean-square vorticity fluctuation. The form of the eddy viscosity (turbulent) equations is based on the realizability constraints; the positivity of normal Reynolds stresses and Schwarz' inequality for turbulent shear stresses. This is not satisfied by either the standard or the RNG κ-ε models which make the realizable model more precise than both models at predicting flows such as boundary layers under strong adverse pressure gradients or separated flows, rotation, recirculation, strong streamline curvature and flows with complex secondary flow features. Finally, a 0.001 tolerance was chosen for the convergence criterion. In terms of the improved changes by Shih et al. (1995), the transport equations become:

$$\frac{\partial}{\partial t}(\rho k)+\frac{\partial}{\partial x_j}(\rho k u_j)=\frac{\partial}{\partial x_j}\left[\left(\mu+\frac{\mu_t}{\sigma_k}\right)\frac{\partial k}{\partial x_j}\right]+G_k+G_b-\rho\varepsilon-Y_M+S_K \quad (1)$$

$$\frac{\partial}{\partial t}(\rho \varepsilon)+\frac{\partial}{\partial x_j}(\rho \varepsilon u_j)=\frac{\partial}{\partial x_j}\left[\left(\mu+\frac{\mu_t}{\sigma_\varepsilon}\right)\frac{\partial \varepsilon}{\partial x_j}\right]+\rho C_1 S\varepsilon-\rho C_2\frac{\varepsilon^2}{k+\sqrt{\nu\varepsilon}}+C_{1\varepsilon}\frac{\varepsilon}{k}C_{3\varepsilon}G_b+S_\varepsilon \quad (2)$$

where G_k represents the generation of turbulent kinetic energy the arises due to mean velocity gradients, G_b is generation of turbulent kinetic energy the arises due to buoyancy, and Y_M represents the fluctuating dilation in compressible turbulence that contributes to the overall dissipation rate. S_ε and S_k are source terms defined by the user. α_k and α_ε are the turbulent Prandtl numbers for the turbulent kinetic energy and its dissipation.

Similar to the previous variations of the *k-ε* models, the turbulent viscosity is determined by the formula given below; however it produces different results as C_μ is not constant.

$$\mu_t=\rho C_\mu\frac{k^2}{\varepsilon} \quad (3)$$

$$C_\mu = \frac{1}{A_0 + A_S \dfrac{kU^*}{\varepsilon}} \tag{4}$$

$$U^* = \sqrt{S_{ij}S_{ij} + \tilde{\Omega}_{ij}\tilde{\Omega}_{ij}} \tag{5}$$

Where $\tilde{\Omega}_{ij} = \overline{\Omega}_{ij} - \varepsilon_{ijk}\omega_k - 2\varepsilon_{ijk}\omega_k$

In the above equation, $\tilde{\Omega}_{ij}$ is the mean rate of rotation tensor viewed in a rotating reference frame with angular velocity ω_k. The constants A_0 and A_S are defined as:

$$A_0 = 4.04 \tag{6}$$

$$A_S = \sqrt{6}\cos\phi \tag{7}$$

Where: $\phi = \frac{1}{3}\cos^{-1}\left(\sqrt{6}\frac{S_{ij}S_{jk}S_{ki}}{\tilde{S}^3}\right)$, $\tilde{S} = \sqrt{S_{ij}S_{ij}}$, $S_{ij} = \frac{1}{2}\left(\frac{\partial u_j}{\partial x_i} + \frac{\partial u_i}{\partial x_j}\right)$

It has been shown that Cμ is a function of the mean strain and rotational rates, the angular velocity of the rotating system, and the turbulent kinetic energy and its dissipation rate. The standard value of Cμ =0.09 is found to be the solution for an inertial sub layer in the equilibrium boundary layer. The constants C1ε, C2, σk and σε have been determined by Shih et al. (1995) and are defined as follows: C1ε =1.44, C2 =1.9, σk =1.0 and σε =1.2.

2.2 Experimental Methods

The electrochemical reactor is formed by arrangement of 14 iron steel ring electrodes, 7 cathodes and 7 anodes, allocated in a sequence of one cathode followed by one anode and separated with a space of 17 mm. Each ring electrode has 137 mm of diameter. The main shaft is driven by a variable speed motor to control the speed of the ring electrode arrangement. The cylindrical tank has a torispherical basis with four baffles arranged symmetrically. Tests were performed at three different electrode rotational speeds, 75 rpm, 150 rpm and 230 rpm. The reactor height was 0.367 m and internal diameter of 0.27 m with four baffles and with a volume capacity of 18 L. The tests were performed in an electrochemical batch reactor with rotating ring electrodes and three different conditions: (a) without impellers, (b) 4-fins and (c) one central PB4 impeller, as shown in Figure 1. Mixing time was evaluated experimentally by using a pulse of a pH known solution and it was defined as the time interval between the pulse of the solution and the moment from which on the measured pH difference remained less than 0.1 per cent of the pH average in the reactor (Kramers et al. 1953).

Different parameters as mass weighted average vorticity magnitude and turbulence intensity were evaluated by using Fluent. In addition the pathlines were obtained for the three cases to have better understanding of the fluid behaviour in the reactor. Figure 2 shows one of the three meshes used during the CFD simulations.

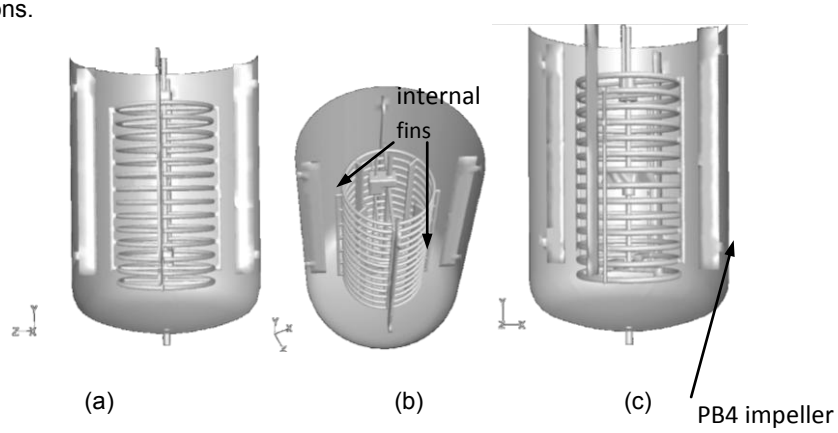

Figure 1: Electrochemical batch reactor with three different conditions: (a) without impellers, (b) internal 4-fins and (c) one central PB4 impeller

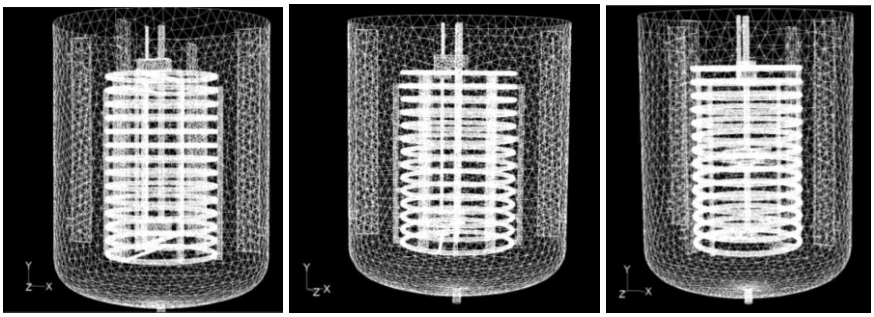

(a) (b) (c)

Figure 2: Electrochemical batch reactor meshes: (a) without impellers, (b) internal 4-fins and (c) one central PB4 impeller

3. Results and discussion

In Figure 3, the pathlines for the three arrangements are shown. It is possible to visualize the flow of the particles in the fluid at the different scenarios. As seen, in the reactor without impellers (a) and in the reactor with 4-fins (b), there are two zones (marked with the doted squares). These zones are not connected, and the fluid behaves as two sections. Therefore, the mixing is poor because the contact between the fluids in both zones is reduced. On the other hand, for the case of and PB4 impeller (c), the flow of the fluid in not divided and it travels form the top to the bottom inside the electrode rings and returns to the top near the walls, producing a better pumping and mixing than the other cases. There are no disconnected zones. Figure 4, shows the contours of the turbulent intensity for the three cases in gray scale. As seen, the highest turbulence intensities inside the rotating ring electrode are reached in the reactor with the PB4 impeller. On the other hand, the lowest turbulence intensity (TI) inside the rotating ring electrode is present when the reactor is operated without impellers. Other important parameter evaluated that improves the mass transfer and mixing is the vorticity. Figure 5, shows the contours of the vorticity magnitude for the three cases. As shown, the vorticity in the three cases is high near the rotating electrode rings. However, the lowest vorticity is present in the reactor without impeller. The vorticity inside the rotating rings zone also is the lowest of the three cases. Although the vorticity increases in the reactor with 4 fins, the increase inside the rotating rings zone, only reaches the zone near the top of the ring electrode. On the other hand, with the reactor with the PB4 impeller, the impeller produces high vorticity in the rotating rings zone, reaching more than the half height of the electrode rings. Table 1, shows the mean turbulent intensity and the mean Vorticity Magnitude at different rpm for the three cases.

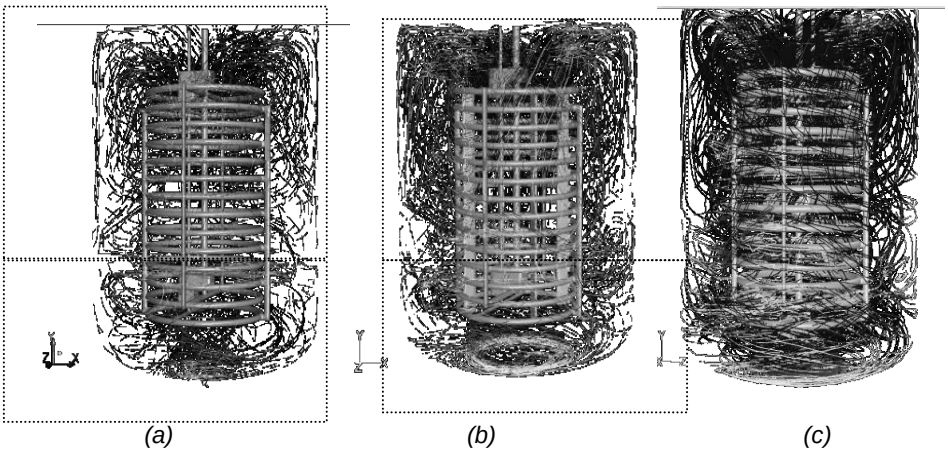

(a) (b) (c)

Figure 3: Pathlines for the reactor; (a) without impellers, (b) 4-fins and (c) PB4 impeller

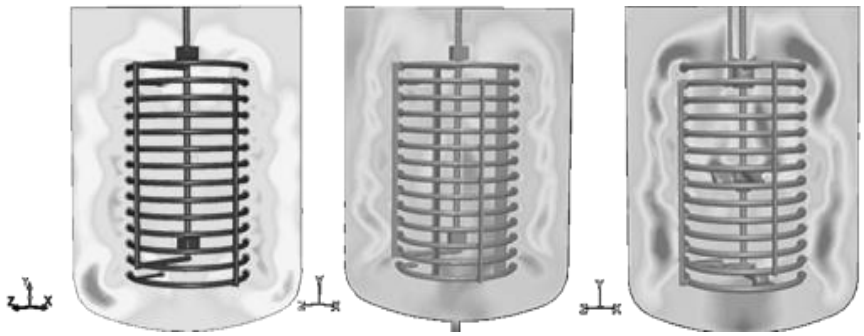

(a) (b) (c)

Figure 4: Contours of the turbulent intensity in the reactor; (a) without impellers, (b) 4-fins and (c) PB4 impeller

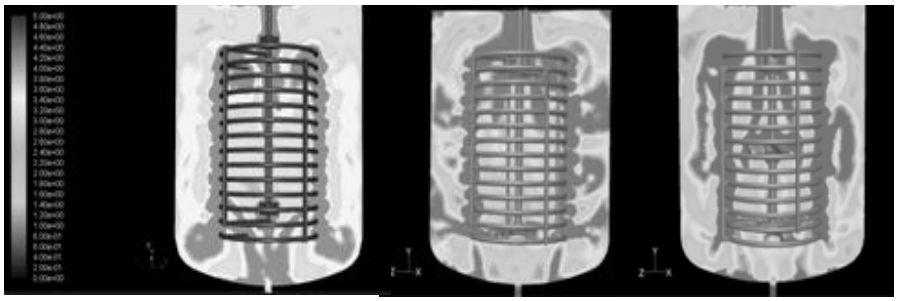

(a) (b) (c)

Figure 5: Contours of the vorticity magnitude in the reactor; (a) without impellers, (b) 4-fins and (c) PB4 impeller

Table 1: Mean Turbulent intensity and Mean Vorticity Magnitude at different rpm for the three cases

	75 rpm			150rpm			230 rpm		
Parameter	Without impellers	4-fins	PB4	Without impellers	4-fins	PB4	Without impellers	4-fins	PB4
Turbulent intensity	0.641	0.649	0. 775	1.18	1.19	1.405	1.887	1.762	1.967
Vorticity magnitude	4.839	5.017	6.380	6.563	6.706	7.335	9.546	9.808	10.627

As shown, the highest values of mean turbulence intensity and vorticity magnitude are presented when the reactor is operated with the PB4 impeller for the three rotational ring electrode speeds. These effects combined, produced that the mixing time were lower in about 52 % with the PB4 impeller and 33 % with the 4 fins, than the mixing time with the reactor operated without impellers with the same power consumption.

4. Conclusions

The impeller types have a very important effect on the hydrodynamic characteristics of the flow. In this work, the PB4 impeller has the best performance of the three scenarios. because with this type of impeller the mixing was improved because the mixing time was reduced until a 52 %, in comparison with the reactor without internal impellers in the rotating ring electrode and in 19 % in comparison with the reactor with four fins. Moreover, the power consumption to reach this improvement was the same than that one for the reactor without impellers.

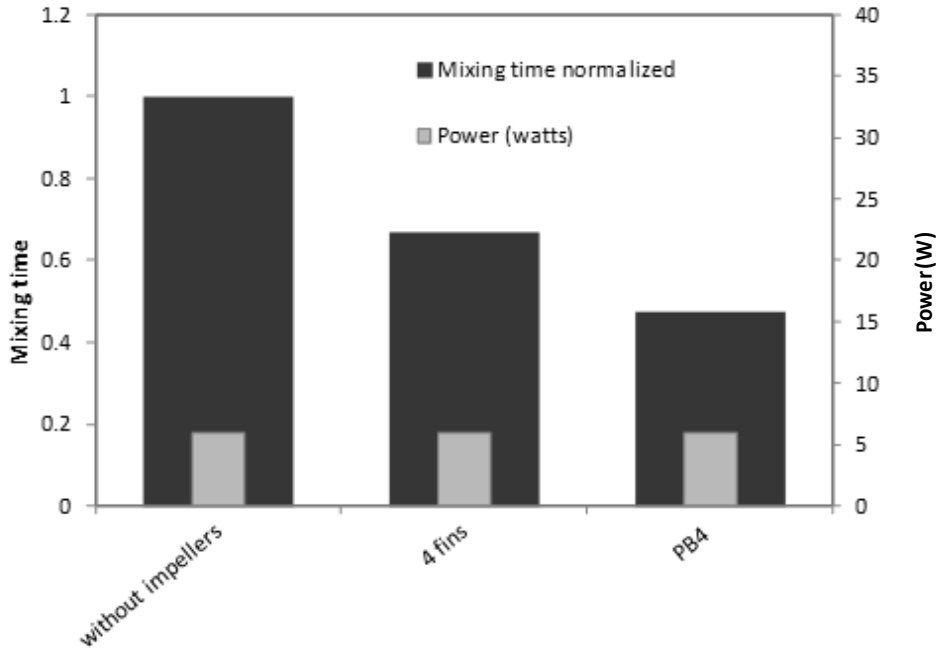

Figure 6: Mixing time and power consumption for the reactor without impellers, 4 fins and PB4 impeller

References

Kramers, H., Baars, G. M. and Knoll, W. H., 1953. A comparative study on the rate of mixing in stirred tanks., Chemical Engineering Science, 2, 35-42.

Martinez, S.A. Rodriguez M.G., Barrera. C., 2000, A kinetic model to describe the removal of Chromium VI from rinsing waters of the metal finishing industry, by electrochemical processes, Water Science and Technology, 42, 55-61.

Martinez, S.A., Mollinedo, H , Mendoza, V., Huerta, O., 2011, Evaluation of the hydrodynamic performance of an electrochemical reactor with rotating ring electrodes using CFD analysis, Chemical Engineering Transactions, 25, 315-320, DOI: 10.3303/CET1125053

Martinez-Delgadillo, S., Mollinedo H., Mendoza-Escamilla V., Gutiérrez-Torres C., Jiménez-Bernal J, Barrera-Diaz C., 2012, Performance evaluation of an electrochemical reactor used to reduce Cr(VI) from aqueous media applying CFD simulation. Journal of Cleaner Production, 34, 120-124

Martínez S.A., Ramírez J., Mollinedo H.R., Mendoza V., Gutiérrez- C. and Jiménez J.,2013, Determination of the Spatial Distribution of the Turbulent Intensity and Velocity Field in an Electrochemical Reactor by CFD, International Journal of Electrochemical Science , 8, 274-289.

Rammohan, A.R., Kemoun, A., Al-Dahhan, M.H., Dudukovic, M.P., 2001. A Lagrangian description of flows in stirred tanks via computer-automated radioactive particle tracking (CARPT). Chem. Eng. Sci. 56, 2629-2639.

Shih, T.H., Liou, W.W., Shabbir, A., Zhu, J., 1995. A new κ-ϵ eddy viscosity model for high Reynolds number turbulent flows. Model development and validation. Computers Fluids 24 (3), 227–238